American Journal of Biochemistry and Biotechnology

Original Research Paper

The Effect of Trilobatin on Bovine Serum Albumin: Interaction Mechanism and Molecular Docking

Yuhan Zhai, Yuqing Zhang, Yaping Li, Haifang Xiao and Yuanda Song

Department of Food Science and Engineering, Colin Ratledge Center for Microbial Lipids, School of Agricultural Engineering and Food Science, Shandong University of Technology, 266 Xincun West Road, Zibo, China

Article history
Received: 01-07-2023
Revised: 30-10-2023
Accepted: 14-11-2023

Corresponding Author's:
Haifang Xiao, Yuanda Song
Department of Food Science and Engineering, Colin Ratledge Center for Microbial Lipids, School of Agricultural Engineering and Food Science, Shandong University of Technology, 266 Xincun West Road, Zibo, China
Email: xiaohaifang@sdut.edu.cn; ysong@sdut.edu.cn

Abstract: Understanding the transport and distribution of small molecules *in vivo* is aided by studying their interactions with proteins. As a natural sweetener, trilobatin possesses several biological activities. However, uncertainty surrounds the trilobatin and Bovine Serum Albumin (BSA) interaction mechanism. In this study, the binding types, number of binding sites and binding constants of trilobatin interaction with BSA were studied by fluorescence spectrometry. The effect of trilobatin on the spatial conformation of BSA was investigated using FT-IR, fluorescence and UV-V is absorption spectra. Moreover, the molecular docking method was employed to research the exact binding model of trilobatin and BSA. Findings from this investigation demonstrated that static quenching was the method by which trilobatin suppressed the fluorescence of BSA. The binding constants Ka of trilobatin and BSA at 298, 304 and 310 K were 2.23×10^4, 3.06×10^4 and 6.39×10^4 moL/L, respectively and only a single site of BSA was bound to trilobatin. According to the discoveries of molecular simulation and thermodynamic analysis, the predominant forces between trilobatin and BSA were hydrogen bond and hydrophobic force ($\Delta H° >0$ and $\Delta S° >0$). Trilobatin and BSA had an endothermic, entropy-driven reaction during their binding contact ($\Delta G° >0$). Additionally, non-radiative energy transfer took place among trilobatin and BSA because their binding distance was smaller than 7 nm. Moreover, trilobatin altered the microenvironment and conformation of BSA and formed the non-fluorescent ground state complex. Important data supporting trilobatin's availability and distribution were supplied by this investigation.

Keywords: Trilobatin, Bovine Serum Albumin (BSA), Interaction, Spectroscopic Method and Molecular Docking

Introduction

Small molecules in the body must interact with large molecules before they exert their physiological or pharmacological properties (Cui *et al*., 2008). Studying the interaction of small molecules with *Biomacromolecules* is not only vital to the biological investigation of small molecule discovery at the molecular level but also advances knowledge of how small molecules are transported and metabolized throughout the body (Yang *et al*., 2016). After small molecules (such as natural products, drugs) enter the biological body, they can only reach the recipient site through the transport and storage of plasma to exert their physiological or pharmacological properties (Wang *et al*., 2009). In animal plasma, the most prevalent carrier protein is serum albumin. Serum albumin transports tiny molecules to the appropriate target organs to carry out the appropriate physiological effects in addition to balancing the blood vessel's internal and external osmotic pressure. Therefore, understanding the *in vitro* transport and metabolism of tiny molecules, along with the process behind tiny molecule metabolism, may be gained from studying how small molecules and serum albumin interact. The two most often utilized models in the investigation of molecule-protein interactions are BSA and Human Serum Albumin (HSA). The amino acid sequences of BSA and HSA are very similar, so

their structure and properties are basically similar and they can extensively bind to many endogenous and exogenous molecules and form complexes to complete the physiological function of plasma (Arques, 2018; Sheinenzon *et al*., 2021; Shojai *et al*., 2022). However, BSA is cheaper and easier to get than HAS.

Trilobatin is a naturally occurring dihydrochalcone that has a high sweetness and low-calorie content (Sun *et al*., 2015). Trilobatin has been proven to have biological actions including anti-inflammatory, antiviral, hypoglycemic and other activities (Gao *et al*., 2018). The storage, transport and biological effects of trilobatin are closely related to its interaction with serum albumin. Consequently, research on the relationship between trilobatin and serum album is required. However, no relevant research has been carried out. Therefore, this study used simulated physiological circumstances (pH = 7.4) to examine the way that trilobatin and BSA bind. The different types of binding forces, the number of binding sites and the binding constants might all be investigated using a fluorescence spectroscope. The impact of trilobatin on BSA's spatial conformation was investigated by FT-IR, synchronous fluorescence and UV-Vis absorption spectra. The trilobatin-BSA exact binding model was studied using molecular docking. The findings of this investigation will give theoretical and empirical support to the pattern of protein and trilobatin interaction and give evidence to help comprehend the trilobatin metabolic pathway.

Materials and Methods

Materials

The supplier of the analytical-grade trilobatin (SKU: PHL83918, purity 98%) and Bovine Serum Albumin (BSA) (SKU: A1933, purity 98%) was Sigma-Aldrich (St Louis, Mo, USA) in this research. Tris-HCl buffer solution (0.1 M) was used to prepare 1.0 μM BSA solution. The 100 μL Dimethyl Sulfoxide (DMSO) used in the experiment dissolved 2.5 mg of trilobatin and diluted it to 5.73 mL with ultra-pure water to obtain 1.0 mM of trilobatin stock solution. And the trilobatin stock solution of trilobatin (1.0 mM) was lowered to the required lesser concentration by the addition of ultra-pure water. The water used in the studies was all ultra-pure and other reagents were all of a high analytical standard.

Fluorescence Spectra Measurement

We measured the BSA fluorescence spectra with a spectrofluorometer (model F-7000, Hitachi, Japan). The emission spectra were recorded between 300 and 450 nm with the excitation wavelength set at 280 nm and excitation slits calibrated at 10 nm. In a nutshell, after continuously titrating trilobatin at final concentrations varying from 0-10-1.0 μM BSA, the reaction between trilobatin and BSA was kept for 5 min. The mixtures were left to equilibrate for 5 min. After that, by recording the fluorescence spectra at 298, 304 and 310 K, respectively, the effects of trilobatin on the fluorescence spectra of BSA at various temperatures were investigated.

The resulting synchronous fluorescence spectra reveal the distinctive fluorescence of Tryptophan (Trp) and Tyrosine residues (Tyr) at $\Delta\lambda$ = 60 nm and $\Delta\lambda$ = 15 nm, respectively (Shi *et al*., 2012). Therefore, under an excitation wavelength of 285 nm and a slit width of 10 nm, the synchronous fluorescence spectra of BSA at $\Delta\lambda$ = 15 nm and $\Delta\lambda$ = 60 nm ($\Delta\lambda = \Delta\lambda_{excitation} - \Delta\lambda_{emittd}$) in the wavelength range of 300-400 nm were scanned, respectively.

In the current investigation, all reported experimental fluorescence readings were adjusted by the following calculation to account for the inner filter effect (Jiang *et al*., 2016):

$$F_C = F_m e^{(A_1+A_2)/2} \quad (1)$$

The abbreviations F_c and F_m represent the corrected and measured fluorescence, respectively. Trilobatin absorbs light differently at emission and excitation wavelengths and the corresponding values are A_1 and A_2, respectively.

UV-Vis Spectra Measurements

We recorded the UV-Vis spectra of mixes using a UV-Vis spectrophotometer (UV-2600, Shimadzu, Japan). Briefly, the combined solutions of BSA (1.0 μ) and trilobatin (0, 2, 4, 8 and 12 μM) were submerged in water at 298 K for 20 min to make the solution temperature equalize and then the UV-Vis spectra (200-450 nm) were obtained.

FT-IR Spectra Measurements

With some changes from the previous procedures (Shi *et al*., 2016), the FT-IR spectra of BSA (1 μM) solution, buffer solution, trilobatin (2 μM) solution and trilobatin-BSA mixed solution were obtained at ambient temperature with a 4 cm^{-1} resolution and wavenumbers ranging from 1700-1600 cm^{-1} by an FT-IR spectrometer (Thermo Nicolet-5700, Nicolet Co., USA), so as to further analyze the effect of trilobatin on the secondary structure of BSA.

Molecular Docking Studies

Utilizing molecular docking software (AutoDock 4.2, USA), the interaction configuration between trilobatin and BSA was examined in this study. The 3D shape of trilobatin was retrieved via the Pubchem data bank (http://pubchem.ncbi.nlm.nih.gov/) and the BSA (Serial number: 4f 5s) crystal structure was downloaded from the protein database (http://www.rcsb.org/pdb)

(Sengottiyan *et al*., 2022). Prior to docking, the BSA's crystal structure was hydrogenated, charged and dewatered using AutoDockTools (ADT) 1.5.6. The lattice points of molecular docking were set as 80 Å×80×90 Å, the spacing of lattice points was 0.375 Å. When two molecules are able to form a tighter bond, they lose less energy and release more energy, which is the minimum binding energy (Agrawal *et al*., 2019). In molecular docking, the minimum binding energy is an important index to evaluate the intermolecular binding ability. Therefore, for further examination, the BSA and trilobatin patterns in the docking data with the lowest binding energies were chosen.

Statistical Analysis

Every experiment was carried out at least three times. Using IMB SPSS statistics 2.0 software, the data were evaluated using one-way Analysis of Variance (ANOVA) and Duncan's multiple comparative analysis. The data were reported as the mean ± Standard Deviation (SD). The differences between the sample mean values were determined using the Least Significant Difference (LSD) test at a significance threshold of 0.05.

Results and Discussion

Fluorescence Quenching Mechanism

The maximal fluorescence emission wavelengths of three fluorescent amino acids (Trp, Tyr and Phenylalanine (Phe)) of protein molecules are 348, 303 and 282 nm, respectively (Khan and Tayyab, 2001). Protein fluorescence is excited at 280 nm and the maximum emission peak at about 340 nm is mainly from Trp residues. Chromophore fluorescence intensity could be reduced by molecular interaction, excited state reaction, collision quenching, molecular rearrangement, formation of ground state complexes and energy transfer (Vijayabharathi *et al*., 2012). The fluorescence quenching experiments looked into the interaction of trilobatin and BSA. In the same settings, trilobatin had no fluorescence absorption whereas BSA showed a sizable peak in its fluorescence emission at 340 nm. Additionally, when trilobatin concentration increased, the fluorescence quench of BSA enhanced (Fig.1 A-C). These findings demonstrate a typical fluorescence quenching phenomenon, suggesting that trilobatin and BSA interacted and formed a faint or non-fluorescent trilobatin-BSA complex.

Fluorescence quenching mechanisms may be classified into two categories: Dynamic quenching and static quenching (Shi *et al*., 2012). Their reliance on viscosity and temperature distinguishes them from one another. The development of non-fluorescent or faintly fluorescent complexes between small molecules and protein molecules results in static quenching, which is a kind of fluorescence quenching. When the temperature increases, the complexes dissociate, resulting in a decrease in the quenching constant. Dynamic quenching is the fluorescence quenching caused by the collision between a small molecule and an excited protein molecule. When the temperature increases, the collision between them intensifies, resulting in the increase of the quenching constant (Yu *et al*., 2012). To assess the fluorescence quenching type of protein by small molecules, the Stern-Volmer equation is typically utilized (Limpouchová and Procházka, 2016):

$$\frac{F_0}{F} = 1 + K_{SV}[Q] = 1 + K_q\tau_0[Q] \quad (2)$$

where, the BSA fluorescence intensities with and without trilobatin are denoted by the letters F and F_0, respectively; the trilobatin concentration is represented by $[Q]$; Ksv (L/moL) stands for the Stern-Volmer quenching constant; a fluorophore without trilobatin has an average lifetime of τ_0 (10^{-8} s) and Kq (L/moL/s) ($Kq = Ksv/\tau_0$) is the symbol for the bimolecular quenching rate constant.

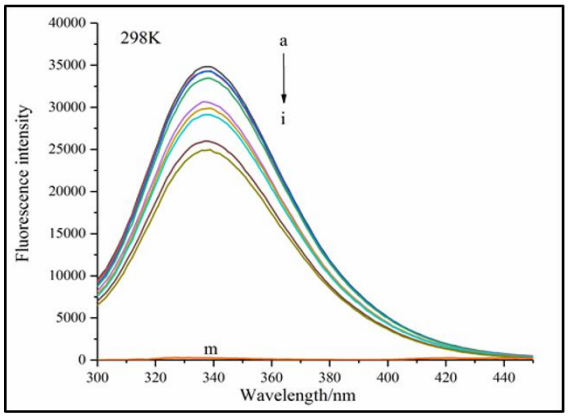

(a)

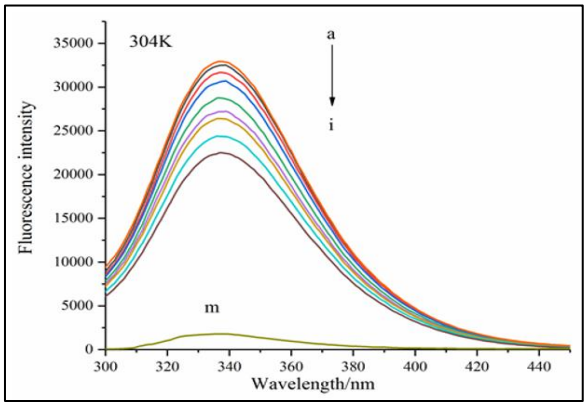

(b)

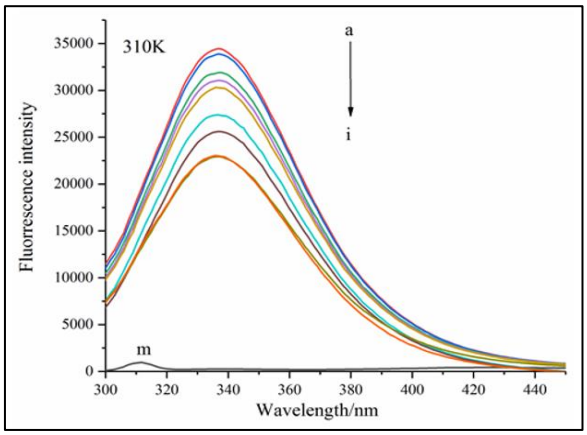

(c)

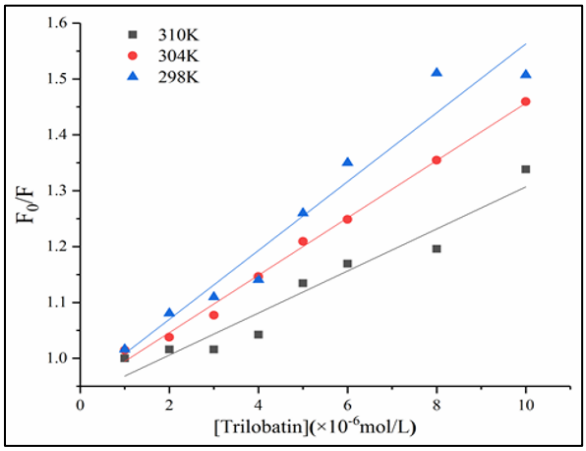

(d)

Fig. 1: Temperature-dependent fluorescence spectra of BSA at pH 6.8, λ ex = 280 nm, with varying trilobatin concentrations. For curves a → i, c (trilobatin) = 0, 1, 2, 3, 4, 5, 6, 8 and 10×10^{-6} moL/L and c (BSA) = 1×10^{6} moL/L, respectively; Curve m, c (trilobatin) = 3.0×10^{6} moL/L showed just the trilobatin emission spectra; (A) 298 K; (B) 304 K; (C) 310 K; (D) Trilobatin induced temperature dependent fluorescence quenching of BSA was shown using Stern-Volmer plots (298, 304 and 310 K)

As illustrated in Fig. 1D, there was only one type of fluorophore in the protein and only one mode of quenching (either dynamic or static) that occurred, according to the Stern-Volmer illustrations at 298, 304 and 310 K, which all showed a beautiful linear link (Soares *et al*., 2007). K_q values were computed and presented in Table 1. Showed that K_{sv} progressively dropped as treatment temperature rose, suggesting that static quenching instead of dynamic quenching may be the process by which trilobatin and BSA interact. Additionally, the highest scattering collision quenching constant of biological macromolecules (2.0×10^{10} L/moL/s) was much smaller than the *Kq* values which were 6.16, 5.13 and 3.76×10^{12} L/mol/s at 298, 304 and 310 K, respectively (Table 1). These findings further demonstrated that trilobatin quenched the fluorescence of BSA, however, it did so in a static way by forming a complex between BSA and trilobatin rather than in a dynamic way through intermolecular collisions.

The following formula was used to get the binding constant (*Ka*) and the number of binding sites (*n*) in the static quenching interaction (Wei *et al*., 2010):

$$lg\frac{F_0-F}{F} = lg\,K_a + n\,lg[Q] \quad (3)$$

where, the fluorescence intensities of *BSA* without or with trilobatin stand for F_0 and F, respectively; the trilobatin concentration is represented by [*Q*]; the binding constant is *Ka* and the number of binding sites on each *BSA* molecule is *n*.

Table 1 listed the values of K_a and *n*, which were determined based on the slope and intercept of the regression curve in Fig. 2A. As the temperature rose, so did the K_a value, but the measurements of *n* at various temperatures were all close to 1, confirmed that the protein-bound by each fluorophore increased and only a single site of BSA was bound to trilobatin.

Thermodynamic Parameters and Binding Forces

In general, the interaction between proteins and small molecules involves many non-covalent forces, including electrostatic, hydrogen bond, van der Waals and hydrophobic interactions (Meng *et al*., 2012). Thermodynamic tests were used to further establish the trilobatin's binding strength with BSA. To determine the free Energy change ($\Delta G°$), Enthalpy change ($\Delta H°$) and Entropy change ($\Delta S°$) of thermodynamic parameters, the formula below was applied (Ross and Subramanian, 1981):

$$\ln\frac{K_{a2}}{K_{a1}} = \frac{1}{R}\left[\frac{1}{T_1}-\frac{1}{T_2}\right]\Delta H \quad (4)$$

$$\Delta G = \Delta H - T\Delta S = -RT\ln K_a \quad (5)$$

The binding constants at T_1 and T_2, are K_{a1} and K_{a2}, respectively. The gas constant is R (8.314 J/moL/K).

The fact that the measurements of $\Delta H°$ and $\Delta S°$ are more than zero indicates that the force is mostly hydrophobic. In situations when the electrostatic force predominates, $\Delta H°$ is lower than zero and $\Delta S°$ is higher than zero. If both $\Delta H°$ and $\Delta S°$ are less than zero, the van der Waals force, or hydrogen bond, is the main force (Wang *et al*., 2012; Zhang *et al*., 2012). As seen in Table 1, $\Delta G°$ was negative at all test temperatures, demonstrating that trilobatin and BSA interacted primarily through an endothermic, entropy-driven reaction and hydrophobic forces were the primary active force between trilobatin and BSA by the fact that both $\Delta H°$ and $\Delta S°$ were positive values.

Combined with the Calculation of Distance

In dynamic quenching, energy transfer between molecules is caused by collisions, while energy transfer occurs even without intermolecular collision in static quenching. Fluorescence quenching is the outcome of non-radiative energy transfer between energy donor and acceptor molecules if their fluorescence emission spectra sufficiently overlap and they are less than 7 nm apart (Baptista and Indig, 1998). It was evident from Fig. 2B, that there was some overlap between the UV absorption spectra of trilobatin and the fluorescence emission spectrum of BSA, which means there might be any energy transfer between the molecules of trilobatin and BSA. The relationship between the acceptor-donor distance and the critical energy transfer distance, which determines the energy transfer Efficiency (E), was as follows (Bi *et al*., 2014):

$$E = \frac{R_0^6}{R_0^6 + r^6} = \frac{F_0 - F}{F_0} \quad (6)$$

where, when trilobatin is absent from BSA, its fluorescence intensity is denoted as F_0; F is the amount of fluorescence that BSA emits when trilobatin is present; The distance at which trilobatin and BSA are bound is called r; the critical distance is R_0. R_0 is determined by the following formula when the energy transfer efficiency is 50% (Bi *et al*., 2014):

$$R_0^6 = 8.79 \times 10^{-25} \kappa^2 N^{-4} \Phi J \quad (7)$$

The spatial direction of the donor (BSA) and acceptor (trilobatin) is indicated by the κ^2. The medium's refraction index is N (For BSA, $\kappa^2 = 2/3$, $\Phi = 0.14$, $N = 1.36$). The following formula was used to find the integral of the area known as J, which is where the fluorescence emission spectra of the donor and the receiver overlap (Bi *et al*., 2014):

$$J = \frac{\sum F(\lambda)\varepsilon(\lambda)\lambda^4 \Delta\lambda}{\sum F(\lambda)\Delta\lambda} \quad (8)$$

where, the fluorescence intensity of the donor at wavelength λ is indicated by the F (λ); the recipient's molar absorption coefficient at wavelength λ is indicated by ε (λ).

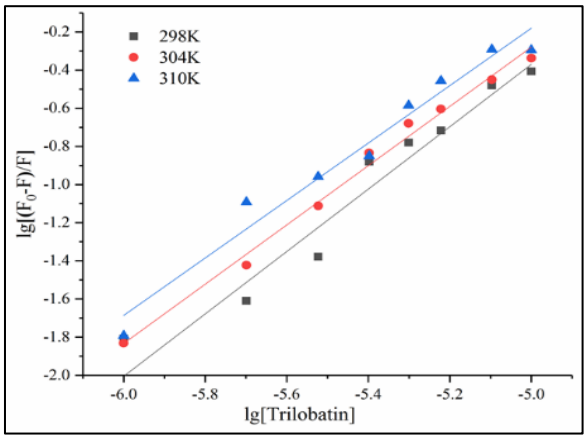

(a)

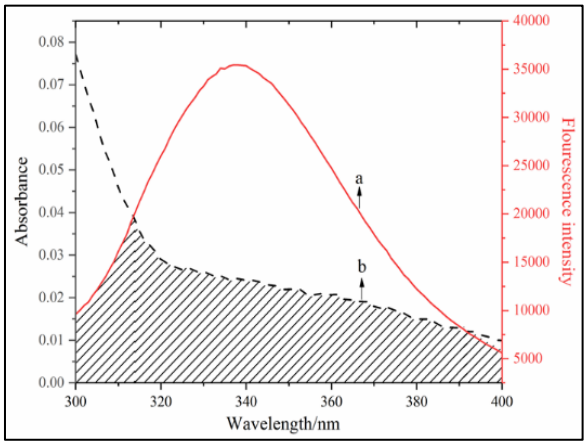

(b)

Fig. 2: (A) Log [(F0-F)/F] against log [Q] for BSA at different temperatures (298, 304 and 310 K): Trilobatin concentration is represented by [Q], where F0 and F represent BSA's fluorescence intensity when trilobatin is absent and present, respectively; (B) The BSA fluorescence spectrum (black) and the trilobatin absorption spectrum (red) at 298 K were overlapped, c (trilobatin) = 3.0×10^{-6} mol/L, c(BSA) = 1×10^{-6} mol/L

Base on formula (6-8), J= 3.41×10^{-15} cm^3 L/mol, R_0 = 2.08 nm, E = 0.3 and r = 2.21 nm. The results showed that the binding distance between trilobatin and BSA was less than 7 nm. In this case, the energy transfer from the donor molecule to the acceptor molecule was completed through intermolecular dipole-dipole resonance coupling between the excited molecule and the acceptor molecule.

Table 1: The number of binding sites N, the quenching and binding constants Kq and Ka and the relative thermodynamic parameters for the interaction of trilobatin with BSA at varying temperatures

T (K)	Kq (×10^{12} moL/L)	Ra	Ka (×10^4 mol/L)	R^b	N	ΔH° (KJ/moL)	ΔG° (KJ/moL)	ΔS° (J/moL/K)
298	6.16±0.00	0.9511	2.23±0.03	0.9683	1.51±0.03		-5.360	461.43
304	5.13±0.00	0.9943	3.06±0.01	0.9910	1.55±0.03	132.14	-7.730	460.10
310	3.76±0.00	0.9382	6.39±0.03	0.9180	1.64±0.03		-16.47	479.39

Conformational Analysis

Synchronous Fluorescence Spectra Analysis

When proteins interact with small molecule active substances, they may cause changes in the fluorescence properties of the system. Amino acid residues that glow in proteins include Tryptophan (Trp) and Tyrosine (Tyr) (Khan and Tayyab, 2001). Since different amino acid residues can only produce fluorescence at their respective excitation wavelengths, the excitation wavelengths can be changed according to different test requirements to obtain different information. In order to represent the microenvironmental changes of amino acid residues including Tyr and Trp in proteins, synchronous fluorescence spectroscopy is frequently utilized (Meti *et al*., 2014). Fluorescence properties of Tyr residues were seen in synchronous fluorescence spectra when the excitation and emission wavelengths were both adjusted to 15 nm. Meanwhile, when the wavelengths were set at 60 nm, synchronous fluorescence spectroscopy may reveal the fluorescence characteristics of Trp residues (Zhao *et al*., 2012). As can be shown in Fig. 3A, trilobatin did not significantly alter the Tyr residue's maximum emission wavelength, suggesting that it had little impact on the Tyr residue's microenvironment. Even though, trilobatin improved the hydrophobicity of Trp residues by changing the microenvironment around them, as evidenced by the faint blue shift in which BSA's maximum emission wavelength decreased after coming into touch with trilobatin (Fig. 3B). Moreover, the fluorescence quenching rate of the interaction between trilobatin and BSA was created by the equation $R_{SFQ} = 1\text{-}F/F_0$. In accordance with the findings of synchronous fluorescence, Fig. 3C demonstrated that trilobatin was closer to Trp than Tyr because the fluorescence quenching rate of BSA at $\Delta\lambda = 60$ nm was greater than that at $\Delta\lambda = 15$ nm.

UV-Vis Spectra Analysis

Using UV-Vis absorption spectra, the structural alterations of BSA upon interaction with triobatin were investigated. Figure 4 illustrates that there was an absorption peak in the vicinity of 280 nm for BSA. With an increase in trilobatin concentration, the BSA's absorption peak migrated from 279-284 nm, demonstrating a clear red shift (the frequency decreased and the wavelength increased). It was reported that the creation of non-fluorescent ground state complexes could alter the protein's absorption spectrum whereas dynamic quenching has no effect on it (Du *et al*., 2012). Therefore, the experiment's outcomes showed that adding trilobatin changed the structure of BSA, the non-fluorescent ground state complex was formed after the interaction of trilobatin and BSA. Once more, it was demonstrated that trilobatin's suppression of BSA's fluorescence was static.

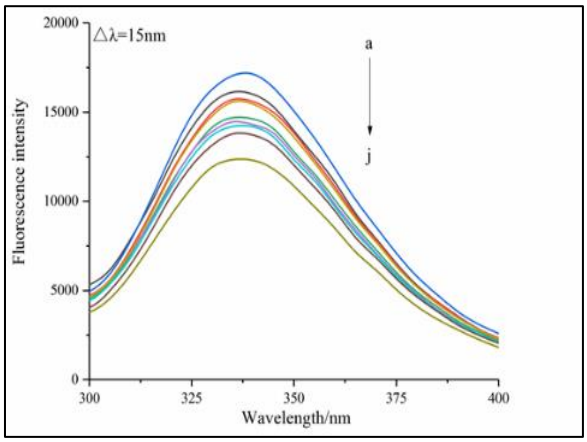

(a)

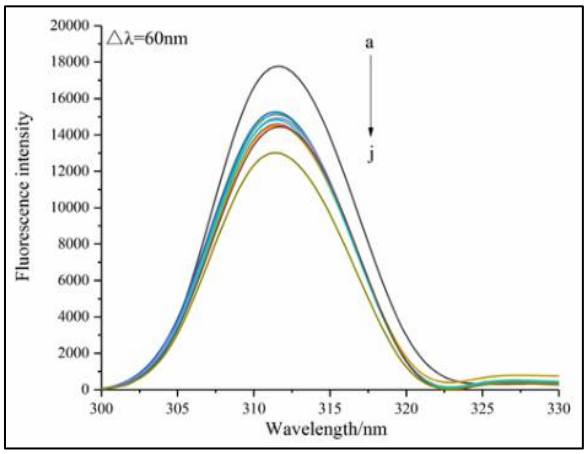

(b)

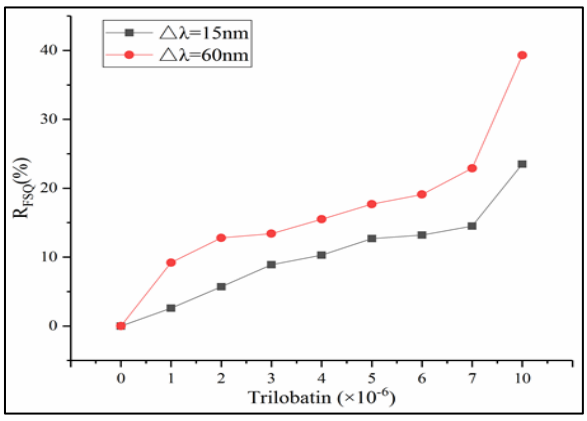

(c)

Fig. 3: BSA's synchronous fluorescence spectra at various concentrations of trilobatin; (A) $\Delta\lambda = 15$ nm; (B) $\Delta\lambda = 60$ nm. For curves a → j, c (trilobatin) = 0, 1, 2, 3, 4, 5, 6, 8 and 10×10^{-6} moL/L and c (BSA) = 1×10^{-6} moL/L, respectively; (C) Influence of trilobatin on the ratios of BSA's Synchronous Fluorescence Quenching (RSFQ)

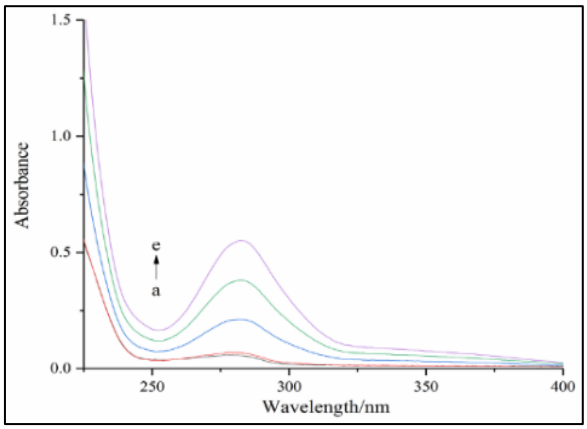

Fig. 4: Trilobatin concentration-dependent BSA UV-Vis absorption spectra. For curves a→ e, c (trilobatin) = 0, 2, 4, 8 and 12×10^{-6} moL/L and c (BSA) = 1×10^{-6} moL/L, respectively

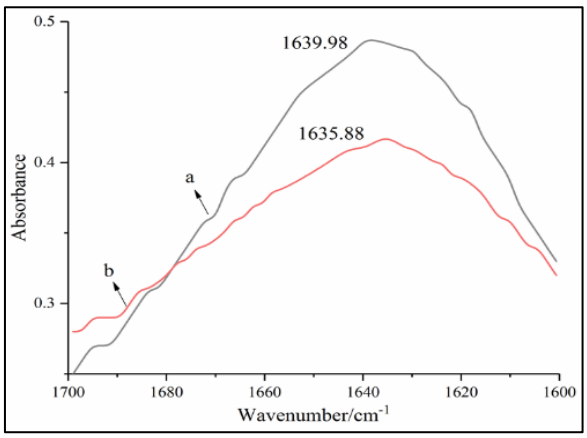

Fig. 5: The trilobatin-BSA complex (b) and free BSA (a) FT-IR spectra. c (BSA) = 1×10^{-6} moL/L and c (trilobatin) = 2.0×10^{-6}moL/L

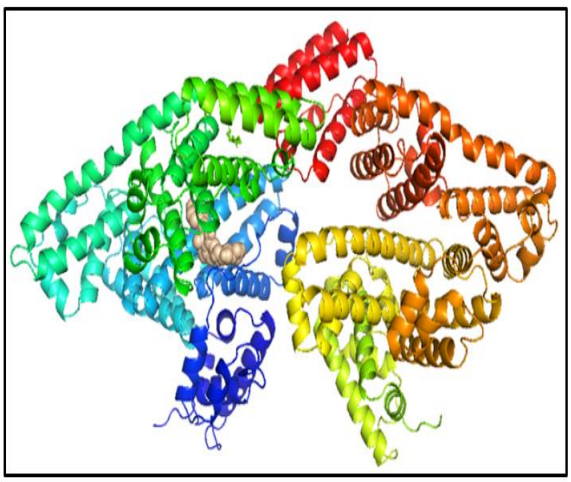

(a)

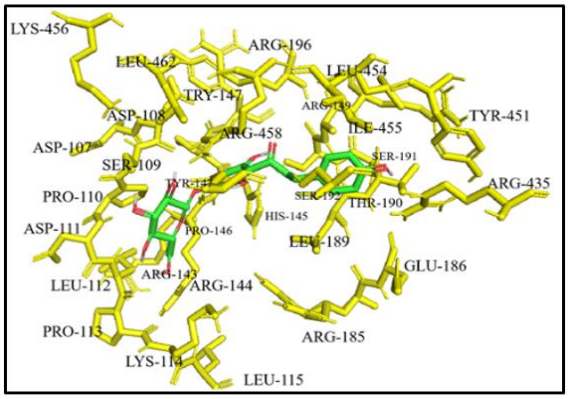

(b)

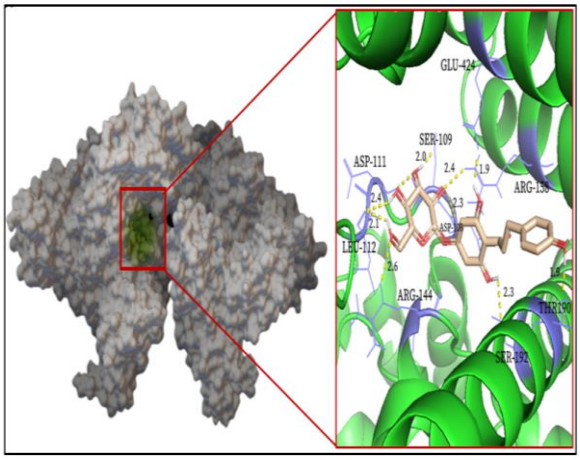

(c)

Fig. 6: Trilobatin's molecular docking with BSA; (A) Location of trilobatin in 3D structure of BSA; (B) Trilobatin was surrounded by residues of BSA; (C) The molecular surface structure (on the left) depicted the binding position of BSA (green domain) interacting with trilobatin; on the right, trilobatin interacted with the amino acid residues around BSA's active site; the hydrogen bonds were indicated by the yellow dashed line

FT-IR Spectra Analysis

Multiple protein amid bands can be seen in FT-IR spectroscopy and distinct amide bands correspond to distinct peptide chain vibration modes. The protein's secondary structure is linked to both the amide I and II bands. The C = O stretching vibration is primarily responsible for the 1600-1700 cm^{-1} number in the amide I band. Amide II possesses C-N stretching vibrations and N-H bending vibrations with a band number of 1500-1600 cm^{-1}. Therefore, the changes in protein amide bands are usually detected by infrared spectroscopy (Zhang *et al*., 2012). Following the interaction among trilobatin with BSA, alterations in the amide band were detected using FT-IR spectra. As

seen in Fig. 5 the peak location of the amide I band changed from 1640-1635 cm^{-1} after the combination of trilobatin and BSA, demonstrating that the interaction between trilobatin and the C=O bond in BSA's secondary structure eventually caused the change of BSA's secondary structure.

Molecular Docking

In the 100 docking cycles between trilobatin and BSA, the model with the least amount of binding energy (-8.27 kcal/moL) was chosen as the final model for additional binding orientation analysis. These results indicated that trilobatin had a greater binding affinity with BSA. Figure 6 displays the theoretical binding mode. Figure 6 trilobatin was obviously easy to enter the active site of BSA. Trilobatin bound with residues of LEU-189 and ALA-193 of BSA in a hydrophobic way. Meanwhile, trilobatin bound with ASP-108, SER-109, ARG-458, LEU-112, ASP-111, GLU-424, ARG-144, SER-192 and THR-190 residues by hydrogen bonding, the yellow dotted line represented hydrogen-bonded and their average was 2.11Å. The outcomes demonstrated that a hydrogen bond acted as the primary interaction between trilobatin and BSA.

Conclusion

The trilobatin and BSA interaction mechanism was investigated in this research utilizing the multispectral method and molecular simulation. The outcomes demonstrated that trilobatin attenuated BSA's intrinsic fluorescence through a static quenching method. And trilobatin had only a single site on BSA. According to thermodynamic parameters, hydrophobia was the primary contact force between trilobatin and BSA. However, due to the intricate nature of the interaction between active molecules and BSA, the interaction is usually a synergistic effect of several forces. Therefore, this study found that hydrogen bond was also involved in the binding of trilobatin and BSA through molecular docking technology. Förster's equation predicts that trilobatin and BSA transmit non-radiative energy through intermolecular dipole-dipole resonance coupling between the excited molecule and acceptor molecule. The findings of multispectral techniques demonstrated that trilobatin altered the microenvironment associated with Trp residues in BSA and decreased hydrophobicity, which caused a shift in BSA's structure. These results provided important theoretical support for the biochemical and physiological processes of trilobatin *in vivo* and were beneficial to the development and utilization of trilobatin in functional foods and drugs. However, due to the diversity and complexity of the protein structure, the interaction between molecules in living organisms must be affected by a variety of coexisting substances in the system. Current research only focuses on the binary system of small molecules-large molecules, which has certain limitations. Therefore, further development should be carried out in future research to improve the detailed information.

Acknowledgment

We extend our gratitude to the publishers for their invaluable assistance in this research. We acknowledge the contributions of the editing team in preparing the manuscript for publication. We appreciate the publishers for providing the resources and platforms for disseminating the findings of our research.

Funding Information

The National Natural Science Foundation of China (No.31972851) and the Taishan industry-leading talent project (No. LJNY201606) provided funding for this study. As a result, we appreciate the financing and support for this study.

Author's Contributions

Yuhan Zhai: Participate in the whole process of experimental designed, experimental process, result analysis and finally written the manuscript.

Yuqing Zhang and Yaping Li: Participated in part of the experiment.

Haifang Xiao: Contributed to the study designed, the interpretation of the results and manuscript preparation.

Yuanda Song: Contributed to the guidance of experimentally designed.

Ethics

There is original content in this piece that hasn't been released before. The corresponding authors (Haifang Xiao and Yuanda Song) attest that every other author has read and accepted the paper and that there are no ethical concerns. The research complies with ethical guidelines and standards.

References

Agrawal, P., Singh, H., Srivastava, H. K., Singh, S., Kishore, G., & Raghava, G. P. (2019). Benchmarking of different molecular docking methods for protein-peptide docking. *BMC Bioinformatics*, *19*(13), 105-124. https://doi.org/10.1186/s12859-018-2449-y

Arques, S. (2018). Human serum albumin in cardiovascular diseases. *European Journal of Internal Medicine*, *52*, 8-12. https://doi.org/10.1016/j.ejim.2018.04.014

Baptista, M. S., & Indig, G. L. (1998). Effect of BSA binding on photophysical and photochemical properties of triarylmethane dyes. *The Journal of Physical Chemistry B*, *102*(23), 4678-4688. https://doi.org/10.1021/jp981185n

Bi, S., Pang, B., Wang, T., Zhao, T., & Yu, W. (2014). Investigation on the interactions of clenbuterol to bovine serum albumin and lysozyme by molecular fluorescence technique. *Spectrochimica Acta Part A: Molecular and Biomolecular Spectroscopy*, *120*, 456-461. https://doi.org/10.1016/j.saa.2013.09.137

Cui, F., Qin, L., Zhang, G., Liu, Q., Yao, X., & Lei, B. (2008). Interaction of anthracycline disaccharide with human serum albumin: Investigation by fluorescence spectroscopic technique and modeling studies. *Journal of Pharmaceutical and Biomedical Analysis*, *48*(3), 1029-1036. https://doi.org/10.1016/j.jpba.2008.07.009

Du, W., Teng, T., Zhou, C. C., Xi, L., & Wang, J. Z. (2012). Spectroscopic studies on the interaction of bovine serum albumin with ginkgolic acid: Binding characteristics and structural analysis. *Journal of Luminescence*, *132*(5), 1207-1214. https://doi.org/10.1016/j.jlumin.2011.12.067

Gao, J., Liu, S., Xu, F., Liu, Y., Lv, C., Deng, Y., ... & Gong, Q. (2018). Trilobatin protects against oxidative injury in neuronal PC12 cells through regulating mitochondrial ROS homeostasis mediated by AMPK/Nrf2/Sirt3 signaling pathway. *Frontiers in Molecular Neuroscience*, *11*, 267. https://doi.org/10.3389/fnmol.2018.00267

Jiang, M., Huang, C. R., Wang, Q., Zhu, Y. Y., Wang, J., Chen, J., & Shi, J. H. (2016). Combined spectroscopies and molecular docking approach to characterizing the binding interaction between lisinopril and bovine serum albumin. *Luminescence*, *31*(2), 468-477. https://doi.org/10.1002/bio.2984

Khan, M. M., & Tayyab, S. (2001). Understanding the role of internal lysine residues of serum albumins in conformational stability and bilirubin binding. *Biochimica Et Biophysica Acta (BBA)-Protein Structure and Molecular Enzymology*, *1545*(1-2), 263-277. https://doi.org/10.1016/S0167-4838(00)00288-0

Limpouchová, Z., & Procházka, K. (2016). Theoretical principles of fluorescence spectroscopy. *Fluorescence Studies of Polymer Containing Systems*, 91-149. https://doi.org/10.1007/978-3-319-26788-3_4

Meng, F. Y., Zhu, J. M., Zhao, A. R., Yu, S. R., & Lin, C. W. (2012). Synthesis of p-hydroxycinnamic acid derivatives and investigation of fluorescence binding with bovine serum albumin. *Journal of Luminescence*, *132*(5), 1290-1298. https://doi.org/10.1016/j.jlumin.2011.12.075

Meti, M. D., Byadagi, K. S., Nandibewoor, S. T., & Chimatadar, S. A. (2014). Multi-spectral characterization and effect of metal ions on the binding of bovine serum albumin upon interaction with a lincosamide antibiotic drug, clindamycin phosphate. *Journal of Photochemistry and Photobiology B: Biology*, *138*, 324-330. https://doi.org/10.1016/j.jphotobiol.2014.05.024

Ross, P. D., & Subramanian, S. (1981). Thermodynamics of protein association reactions: Forces contributing to stability. *Biochemistry*, *20*(11), 3096-3102. https://doi.org/10.1021/bi00514a017

Sengottiyan, S., Malakar, K., Kathiravan, A., Velusamy, M., Mikolajczyk, A., & Puzyn, T. (2022). Integrated approach to interaction studies of pyrene derivatives with bovine serum albumin: Insights from theory and experiment. *The Journal of Physical Chemistry B*, *126*(21), 3831-3843. https://doi.org/10.1021/acs.jpcb.2c00778

Sheinenzon, A., Shehadeh, M., Michelis, R., Shaoul, E., & Ronen, O. (2021). Serum albumin levels and inflammation. *International Journal of Biological Macromolecules*, *184*, 857-862. https://doi.org/10.1016/j.ijbiomac.2021.06.140

Shi, J. H., Pan, D. Q., Jiang, M., Liu, T. T., & Wang, Q. (2016). Binding interaction of ramipril with Bovine Serum Albumin (BSA): Insights from multi-spectroscopy and molecular docking methods. *Journal of Photochemistry and Photobiology B: Biology*, *164*, 103-111. https://doi.org/10.1016/j.jphotobiol.2016.09.025

Shi, Y., Liu, H., Xu, M., Li, Z., Xie, G., Huang, L., & Zeng, Z. (2012). Spectroscopic studies on the interaction between an anticancer drug ampelopsin and bovine serum albumin. *Spectrochimica Acta Part A: Molecular and Biomolecular Spectroscopy*, *87*, 251-257. https://doi.org/10.1016/j.saa.2011.11.048

Shojai, S., Haeri Rohani, S. A., Moosavi-Movahedi, A. A., & Habibi-Rezaei, M. (2022). Human serum albumin in neurodegeneration. *Reviews in the Neurosciences*, *33*(7), 803-817. https://doi.org/10.1515/revneuro-2021-0165

Soares, S., Mateus, N., & De Freitas, V. (2007). Interaction of different polyphenols with Bovine Serum Albumin (BSA) and Human Salivary α-Amylase (HSA) by fluorescence quenching. *Journal of Agricultural and Food Chemistry*, *55*(16), 6726-6735. https://doi.org/10.1021/jf070905x

Sun, Y., Li, W., & Liu, Z. (2015). Preparative isolation, quantification and antioxidant activity of dihydrochalcones from sweet tea (*Lithocarpus Polystachyus Rehd*.). *Journal of Chromatography B*, *1002*, 372-378. https://doi.org/10.1016/j.jchromb.2015.08.045

Vijayabharathi, R., Sathyadevi, P., Krishnamoorthy, P., Senthilraja, D., Brunthadevi, P., Sathyabama, S., & Priyadarisini, V. B. (2012). Interaction studies of resistomycin from streptomyces aurantiacus AAA5 with calf thymus DNA and bovine serum albumin. *Spectrochimica Acta Part A: Molecular and Biomolecular Spectroscopy*, *89*, 294-300. https://doi.org/10.1016/j.saa.2011.12.072

Wang, Q., Zhang, X., Zhou, X., Fang, T., Liu, P., Liu, P., ... & Li, X. (2012). Interaction of different thiol-capped CdTe quantum dots with bovine serum albumin. *Journal of Luminescence*, *132*(7), 1695-1700. https://doi.org/10.1016/j.jlumin.2012.02.016

Wang, T., Zhao, Z., Zhang, L., & Ji, L. (2009). Spectroscopic studies on the interaction between troxerutin and bovine serum albumin. *Journal of Molecular Structure*, *937*(1-3), 65-69. https://doi.org/10.1016/j.molstruc.2009.08.015

Wei, X. L., Xiao, J. B., Wang, Y., & Bai, Y. (2010). Which model based on fluorescence quenching is suitable to study the interaction between trans-resveratrol and BSA? *Spectrochimica Acta Part A: Molecular and Biomolecular Spectroscopy*, *75*(1), 299-304. https://doi.org/10.1016/j.saa.2009.10.027

Yang, L., Zhang, J., Che, X., & Gao, Y. Q. (2016). Simulation studies of protein and small molecule interactions and reaction. *Methods in Enzymology*, *578*, 169-212. https://doi.org/10.1016/bs.mie.2016.05.031

Yu, X., Yang, Y., Zou, X., Tao, H., Ling, Y., Yao, Q., ... & Yi, P. (2012). Study on the interaction between novel spiro pyrrolidine and bovine serum albumin by spectroscopic techniques. *Spectrochimica Acta Part A: Molecular and Biomolecular Spectroscopy*, *94*, 23-29. https://doi.org/10.1016/j.saa.2012.03.050

Zhang, G., Ma, Y., Wang, L., Zhang, Y., & Zhou, J. (2012). Multispectroscopic studies on the interaction of maltol, a food additive, with bovine serum albumin. *Food Chemistry*, *133*(2), 264-270. https://doi.org/10.1016/j.foodchem.2012.01.014

Zhao, X. N., Liu, Y., Niu, L. Y., & Zhao, C. P. (2012). Spectroscopic studies on the interaction of bovine serum albumin with surfactants and apigenin. *Spectrochimica Acta Part A: Molecular and Biomolecular Spectroscopy*, *94*, 357-364. https://doi.org/10.1016/j.saa.2012.02.078